European Journal of Technique

journal homepage: https://dergipark.org.tr/en/pub/ejt

Vol.14, No.2, 2024

Research Article

Microstructure and Mechanical Properties of Cold Metal Transfer Welded AA6013/SiC Metal Matrix Composites

Arzum Isitan[1*], Dirim Bartug Gokturk[2] and Volkan Onar[3]

[1*]Pamukkale University, Mechanical Engineering Department, 20160, Kınıklı, Denizli, Turkey. (e-mail: aisitan@pau.edu.tr).
[2] Pamukkale University, Automotive Engineering Department, 20160, Kınıklı, Denizli, Turkey. (e-mail: dream.gokturk@gmail.com)
[3] Pamukkale University, Mechanical Engineering Department, 20160, Kınıklı, Denizli, Turkey. (e-mail: vonar@pau.edu.tr).

ARTICLE INFO

Received: Sep., 44. 2023
Revised: Nov., 03. 2023
Accepted: Apr, 02. 2024

Keywords:
Composite
Welding
Cold Metal Transfer
Metal Matrix Composite
Heat Input

Corresponding author: *Arzum Işıtan*

ISSN: *2536-5010* | e-ISSN: *2536-5134*

DOI: https://doi.org/10.36222/ejt.1365379

ABSTRACT

This study aims to investigate the impact of varying heat input, achieved through changes in welding current, on the strength of cast composites. Three AA6013 matrix composites (AMCs) of varying SiC content (3, 6, and 9 wt.%) were prepared using the vortex-route method, with dimensions of 250x110x60 mm. Subsequently, the cast composites were sliced into 3.5x100x50 mm dimensions for butt welding. Welding operations were conducted at current intensities of 110 A, 120 A, and 130 A via the cold metal transfer (CMT) welding method. The microstructures and tensile strength of the welded composites were thoroughly analysed.

Results indicated that an increase in heat input led to a decrease in the strength values of welded composites by up to 10%. Furthermore, a notable enhancement in the mechanical properties of the reinforced composites, ranging from 19% to 32%, was observed when compared to the unreinforced alloy. In conclusion, the CMT method, which provides relatively less heat input compared to other welding methods, enables the welding of AMCs to achieve superior mechanical properties while maintaining a low reinforcement ratio.

1. INTRODUCTION

The strength of aluminum alloys tends to decrease at higher temperatures, despite their inherent benefits such as their high fracture toughness and lightweight design. Conversely, ceramic materials exhibit excellent creep resistance and high temperature strength but often lack thermal shock resistance and fracture toughness. To overcome these limitations and create materials with superior thermal and mechanical properties, aluminum matrix and ceramic-reinforced composite materials (AMCs) have been developed. These materials find extensive application areas, particularly in industries like automotive and defense [1].

AMCs, fortified with ceramic particles, outperform non-reinforced alloys in various aspects, including strength-to-weight ratio, dimensional stability, elevated creep and wear resistance, and robust mechanical load-carrying capability [1-4]. With the increasing utilization of AMCs, there is a growing emphasis on research into joining methods, particularly welding technology.

While traditional arc welding techniques remain prevalent due to their widespread use and cost-effectiveness, solid-state welding methods have proven successful in joining AMCs. Despite its excellent metallurgical qualities, solid-state welding faces limitations in mass production, primarily due to constraints in component geometry [5]. This is where techniques like Tungsten Inert Gas (TIG), Metal Inert Gas (MIG), and laser welding come to the fore, offering cost-effectiveness, suitability for mass production, and flexibility with minimal component geometry restrictions. However, welding of AMCs reinforced with ceramic particles using these methods can lead to unintended consequences due to high heat input, particularly in the weld pool, and the substantial thermal expansion of aluminum [3,6].

In the contemporary landscape, Cold Metal Transfer (CMT), integrated into the MIG welding process, stands out as a solution that provides precise power supply control, minimizing thermal input. Unlike traditional MIG welding, where the wire electrode advances until a short circuit occurs, causing high heat input, CMT regulates material transfer using mechanically assisted methods while controlling the start and length of the short circuit. This technique is applicable to various metals and thicker materials, offering advantages in preventing undesired microstructure and precipitate formation caused by high heat input [7,8]. The fundamental principle behind CMT is the short circuit (immersion metal transfer),

patented by Fronius in 2004 [9]. It is envisioned using CMT, a large amount of heat input experienced with traditional arc welding is unlikely to result in a deterioration of the mechanical qualities in the welding area. Due to the minimal heat input, welding of thin sheets and plates together can provide high-quality results. The main distinction between CMT welding and conventional gas metal arc welding is that the latter uses an automation system to regulate the quantity of thermal input, arc length, current, and voltage, as well as the amount of metal transferred [10]. The primary novelty is that the servomotor included in the cannon retracts the wire electrode and aids in the transfer of drops. This servomotor can oscillate up to 70 Hz when a short circuit occurs and operates on alternating current. As a result, the temperature input is significantly reduced, and metal is moved to the weld pool without the use of electromagnetic force. The welding cycle continues after the drop transfer, the arc is ignited, and the wire electrode is advanced once more. Because of the short arc periods, the method's name uses the word "cold" to denote the fact that less heat is used than with MIG or MAG welding methods [9,10].

In the literature, there are very few studies on CMT welding of SiC-reinforced aluminum alloys. Liu et al. (2022) selected the ER5087 (Al-Mg4.5) wire as raw filler and 5A06 Al plate as substrate material. Four different SiC concentrations of Al-Mg alloy deposited on the 5A06 Al plate, and the mechanical properties of Al-Mg alloy improved [11]. Fan et al. (2023) investigated the effect of coating submicron sized La_2O_3 particles on the CMT welded joints of 6061 aluminum alloy [12]. Considering the potential and importance of the use of SiC-reinforced AMCs and the difficulties in the welded joints, there is a lack of studies on CMT welding of AMCs.

In this study, 3%, 6% and 9% in wt. SiC powder was added to the AA6013 alloy, respectively, and composites were produced by the vortex-route casting method. Welded joining processes were carried out by adjusting three different welding current intensities via the CMT method. The microstructures and mechanical properties of welded composite samples were investigated.

2. MATERIAL and METHODS

In this study, AA6013 alloy (AlMg1Si0,8CuMn) was chosen as the matrix material due to its medium strength, high corrosion resistance, good machinability, and widespread preference in welded joints [13]. Its selection was based on qualities such as good weldability, a wide range of industrial applications, and suitability for usage in the automotive sector. The alloy's chemical composition, as well as its physical and mechanical characteristics, are displayed in Tables I and II [14].

TABLE I
THE CHEMICAL COMPOSITION OF AA 6013 ALUMINUM ALLOY

Element	Si	Fe	Cu	Mn	Mg	Cr	Zn	Ti	Al
By weight (%)	0,8	0,25	0,85	0,5	1	0,05	0,12	0,05	Bal.

When creating composite materials with aluminum matrix and ceramic particle reinforcement, SiC is one of the most frequently used materials as the reinforcing ceramic particle. The choices made are significantly influenced by the affordability of SiC particles and their superior wettability by aluminum alloys [1]. For these reasons, SiC ceramic particles with an F1000 size were used as a reinforcement in this study. The SiC powders were subjected to heating in an electric furnace at 200 °C for an hour to evaporate the particles' moisture.

TABLE II
PHYSICAL AND MECHANICAL PROPERTIES OF AA 6013

Symbol	Property	Value
ρ	Density	2,72 g/cm^3
T	Melting Temperature	579 °C
α	Coefficient of Thermal Expansion	21,7x10^{-6} K^{-1}
E	Modulus of Elasticity	71 GPa
Re	Yield Strength	350 MPa
Rm	Ultimate Strenght	400 MPa
A	Elongation at Break	13 (%)
HV	Hardness	115 HV

AMCs can be produced using the same casting techniques that are typically used for aluminum alloys. One such method is vortex-route casting, intended to guarantee the uniform distribution of the reinforcing material in the molten matrix material. The density of the ceramic reinforcement material is higher than that of the aluminum matrix material (Al 2.7 g/cm^3, SiC 3.2 g/cm^3). A stainless-steel mixer combined with an induction furnace was used to prevent SiC particles from aggregating when wet by the aluminum material and to prevent the melt from settling at the bottom of the crucible. The mixing process was conducted slowly to avoid vortex formation.

AMCs were produced by melting the AA 6013 alloy, offered in rod and cylinder shapes, in the casting furnace. The amount of material to be melted is calculated by considering the volume of the model in the sand mold, the volume of the runner parts, and possible losses. Subsequently, the required quantity of AA 6013 alloy was placed into the ceramic crucible within the Nevola Efe series EVO 770 type induction furnace. After cleaning off the slag from the melt's surface and adding the degassing powder to the furnace, which was then heated to 750 °C, reinforcement material was added. A prolonged blending process was approximately 1 hour, was applied to combine SiC and molten aluminum alloy into a homogeneous slurry. Three different composites were obtained by adding 3%, 6% and 9% in wt. SiC powder separately in mixing processes.

Sand molding was used to create casting composite materials in the form of a billet with dimensions of 250x110x60 mm due to its simplicity, speed, and economic efficiency. Figure 1 illustrates the casting furnace, the sand mold, and the resulting cast composite.

Figure 1. The casting furnace, the sand mold, and the cast composite

After the composite billets were produced, a 5 mm layer of chips was removed from all surfaces using a milling machine.

Subsequently, the billets were cut into dimensions of 3.5x100x50 mm using a saw, obtaining the samples necessary for the welding process. Figure 2 represents the chip removal process during milling and cutting of the composite.

Figure 2. The chip removal process and cutting of the composites

The 3.5 mm thick samples were butt welded via CMT welding technique, a novel MIG welding method developed by Fronius International. Welding operations were carried out at Fronius International Istanbul. In the welding process, ER4043 (AlSi5) welding wire with a diameter of 1.2 mm was utilized. The chemical composition of the ER4043 welding wire is provided in Table III. Argon served as the shielding gas at a flow rate of 12 l/min.

TABLE III
THE CHEMICAL COMPOSITION OF ER4043 (ALSI5) WELDING WIRE

Element	Si	Fe	Cu	Mn	Zn	Ti	Al
By weight (%)	4.5-5.5	<0. 5	<0.3	<0.05	<0.1	<0.01	Bal.

Three different current intensities, namely 110, 120, and 130 A, were applied to weld the samples reinforced with 3%, 6%, and 9% SiC. Heat input (H.I.) ($J \cdot mm^{-1}$) generated during the welding operations was calculated using Equation 1, where I is the current intensity (Amperes), V is the voltage (V), η is the arc efficiency (0.8 for CMT method operation), and FR is the feed rate ($mm \cdot min^{-1}$). The welding parameters of all the samples are detailed in Table 4.

$$HI = (60.\mathrm{I}.\mathrm{V})/(\mathrm{FR}).\mathrm{h} \quad (1)$$

TABLE IV
WELDING PARAMETERS

	Material	Current (A)	Voltage (V)	Heat input ($kJ \cdot mm^{-1}$)
1	*AA6013*	110	14.2	0.12
2	*AA6013*	120	14.4	0.13
3	*AA6013*	130	14.8	0.14
4	*AA6013+3% SiC*	110	14.2	0.12
5	*AA6013+3% SiC*	120	14.4	0.13
6	*AA6013+3% SiC*	130	14.8	0.14
7	*AA6013+6% SiC*	110	14.2	0.12
8	*AA6013+6% SiC*	120	14.4	0.13
9	*AA6013+6% SiC*	130	14.8	0.14
10	*AA6013+9% SiC*	110	14.2	0.12
11	*AA6013+9% SiC*	120	14.4	0.13
12	*AA6013+9% SiC*	130	14.8	0.14

Following the welding procedure, tensile test specimens were made by cutting flat bars measuring 3.5x20x140 mm into three pieces for each reinforcement ratio. Tensile tests were conducted in the Mechanical Engineering Materials Laboratory at Pamukkale University using a 30-ton Alşa brand tensile test machine, completed at a speed of 20 mm/min.

In the Metallography Laboratory of the Pamukkale University Mechanical Engineering, samples of non-reinforced alloy and reinforced composite materials, joined under different welding conditions, underwent examination. Their microstructure and macrostructure were analyzed using a microscope. The composites were further characterized using a Schottky Field Emission Scanning Electron Microscope (FESEM) in high vacuum mode (HV) (10^{-6} mbar) at the Pamukkale University Advanced Materials Research Center (ILTAM).

Phase analyses of the welded SiC reinforced composites were performed at Afyon Kocatepe University Technology Application and Research Center (TUAM) using a X-ray spectroscopy (XRD) Bruker D8 Advance diffractometer.

3. EXPERIMENTAL RESULTS

3.1. Tensile Test Results

Tensile strength (Rm) and yield limit (Re) values of welded samples are shown in Table V. Almost all samples fractured at weld seam. The mechanical characteristics of the unreinforced as-cast AA 6013 alloy were determined to be Rm=83.73 MPa and Re=67 MPa. The highest values after the welding process were obtained as Rm=76.3 MPa and Re=60.2 MPa at 130 A for the unreinforced AA 6013 alloy. Rm and Re both decreased by 9% and 11% in the specimen with welding process in order.

TABLE V
THE CHEMICAL COMPOSITION OF ER4043 (ALSI5) WELDING WIRE

	Material	Current (A)	Heat input ($kJ \cdot mm^{-1}$)	Rm (MPa)	Re (MPa)
1	*AA6013*	110	0.12	70.6	57.8
2	*AA6013*	120	0.13	58.3	54.9
3	*AA6013*	130	0.14	76.3	60.2
4	*AA6013+3% SiC*	110	0.12	100.56	83.46
5	*AA6013+3% SiC*	120	0.13	95.09	80.9
6	*AA6013+3% SiC*	130	0.14	90.9	75.83
7	*AA6013+6% SiC*	130	0.14	73.88	60.3
8	*AA6013+9% SiC*	110	0.12	96.01	82.36
9	*AA6013+9% SiC*	120	0.13	95.19	80.9
10	*AA6013+9% SiC*	130	0.14	93.47	79.22

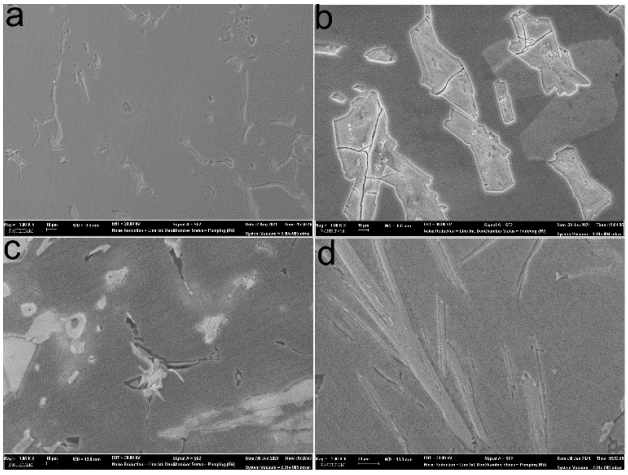

Figure 3. FESEM images of cast unreinforced alloy (a), 3% SiC (b), 6% SiC (c), and 9% SiC (d) reinforced composite materials

As a result of the tensile test, the highest average tensile strength value, Rm=100.56 MPa, was obtained at 110A welding current of AA6013+ 3% SiC composite. As the intensity of the current increased in the CMT method welding of AA6013+ 3% SiC composite, the strength values decreased by up to 10%.

Similar result is valid for 9% SiC reinforced composite. The highest average tensile strength value, Rm=96.01 MPa, was obtained at 110A welding current of AA6013+ 9% SiC composite. While the effect of heat input is more obvious in the 3% SiC reinforced composite, the reduction effect is less in the 9% SiC reinforced composite.

The tensile result values of welded joints of AA6013+ 6% SiC composite could not be obtained exactly. As can be seen in Figure 8, it is thought that the reason for this is the cracks and voids formed in the base metal alloy, transition zone, and welding area, which are caused by unsuitable casting conditions and the formation of a dendritic structure in the welding area.

In contrast to the unreinforced alloy, the mechanical values obtained at all reinforcement ratios decreased as the welding current and heat input increased.

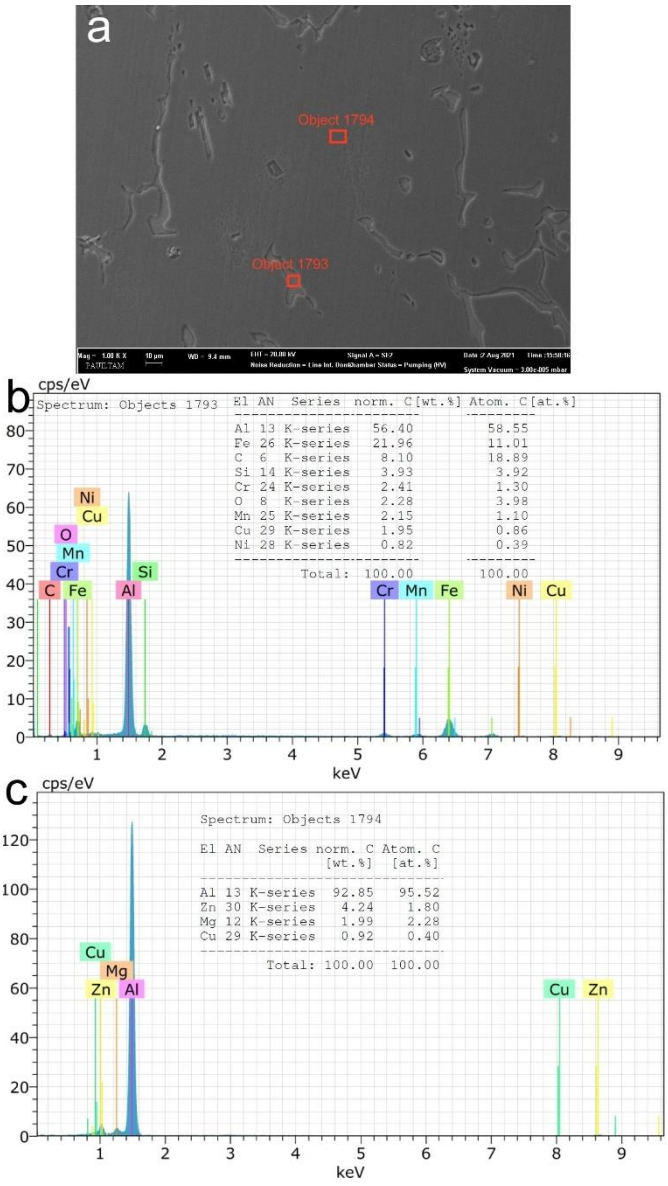

Figure 4. FESEM point analyses of unwelded AA6013 alloy

3.2. Macro and Microstructure Results

In Figure 3, FESEM images of cast unreinforced alloy (a), 3% (b), 6% (c), and 9% (d) reinforced composite materials can be shown, respectively.

Although there are alloying elements such as Si, Fe, Cu, Mn, Mg, Zn, and Ni in the AA 6013 alloy, as can be seen in Figure 4c, mainly Zn, Mg, and Cu were detected in the matrix structure in the FESEM point analysis (object 1794). In the point (object 1793) marked with red mark, Si, Fe, Cr, Cu, Mn, Mg, Zn, Ni, and C were detected (Figure 4b).

Gaps were detected in the weld seam and transition zone (HAZ) images of unreinforced AA 6013 alloy joined at 110 A (Figure 5). In the unreinforced AA 6013 alloy welded at 120 A, weld penetration was achieved as the welding current increased, and it was determined that there were fewer and smaller diameter gas voids compared to the sample joined with 110 A (Figure 6).

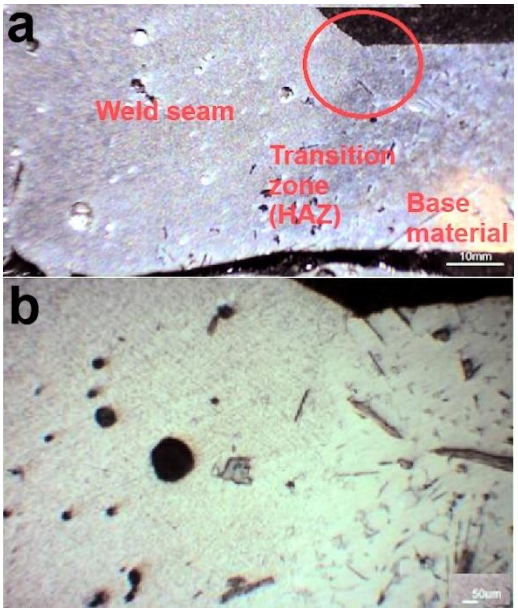

Figure 5. Macrostructure (a) and microstructure (b) images of unreinforced AA 6013 alloy joined at 110 A

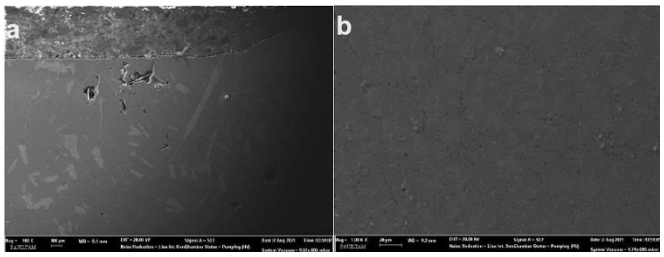

Figure 6. FESEM images of unreinforced AA 6013 alloy joined at 120 A: a) HAZ, b) Weld seam

Figure 7 shows the FESEM microstructure and point analysis of 3% SiC reinforced AMC as-cast condition. It was observed that SiC powders dispersed in all three composites without agglomeration. In Figure 7, red arrows indicate some of SiC particles. A point analysis of the structure (Figure 7b, Object 2431) shows that around the powders, thick rod-like structures consisting of Fe, C, O, Zn, Mg, and Si were formed. The thin and long rod-like structures, some of which are marked with a blue arrow, were observed to be β-Al_5FeSi platelets, similar to studies in the literature [15,16]. The primary silicon structures are marked with a green arrow, Mg_2Si structures are marked

with an orange arrow, and the purple arrow marks the Al_2Cu structures formed, similar to studies in the literature [16,17].

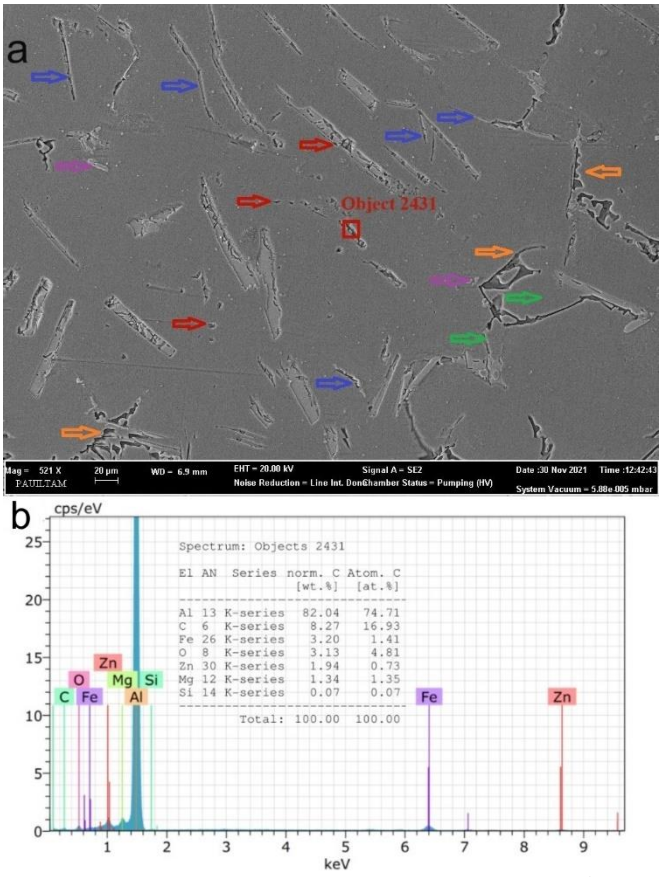

Figure 7. FESEM microstructure (a) and a point analysis (b) of 3% SiC reinforced alloy as-cast condition.

Since the highest tensile strength values were obtained at 110 A welding current, FESEM analysis of these specimens was performed for SiC reinforced composites. The microstructure image and FESEM line analysis of AA6013+ 3% SiC composite welded at 110 A welding current are shown in Figure 8. In the point analyses performed in the transition zone, the complex structures consisting of Fe, Cr, Mn, O, Mg, Mg, Zn, and Mn in the microstructure formed from the HAZ towards the weld seam were replaced by Al-Zn and SiC particles oriented towards the weld seam.

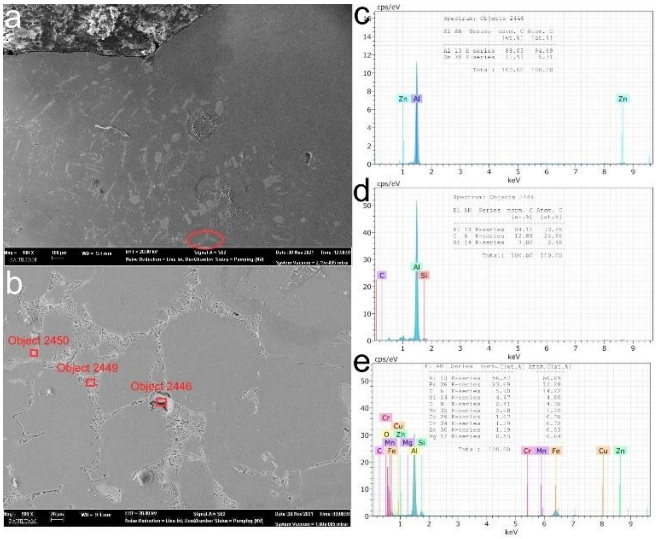

Figure 8. The FESEM microstructure images (a), (b), and FESEM point analyses (c), (d), and (e) of AA6013+ 3% SiC composite welded at 110 A

In the welded joints of AA6013+ 6% SiC composite, very large amount of cracks and gaps were detected in the base metal, transition zone, and welding area under all heat input values. Figure 9 presents of AA6013+ 6% SiC composite welded at 110 A FESEM microstructure of HAZ (Figure 9a), weld seam (Figure 9b), and FESEM weld seam area analysis. In the FESEM area analysis structures containing C, O, Zn, and Fe were predominantly detected in the unwelded samples, while O, Mg, Zn, Fe, Cr, and Si were predominantly detected in the transition zone line analysis of the welded samples (Figure 8a). In the point and area analyzes performed in the transition zone and source region, formations with Fe, C, Cr and Si contents were detected in the transition zone and dendritic formations with C, O, Fe, Si and Mg contents were detected in the source region (Figure 9c).

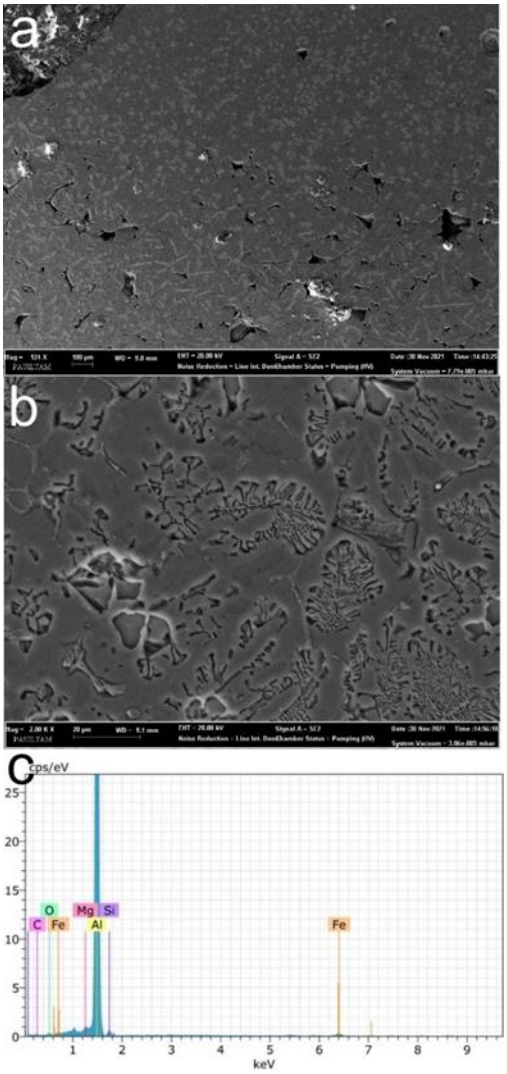

Figure 9. The FESEM HAZ image (a), weld seam microstructure image (b), and weld seam FESEM area analysis of AA6013+ 6% SiC composite welded at 110 A.

Gaps and cracks were detected in the weld and transition areas of AA6013+ 9% SiC composite. In the weld seam FESEM area analysis, structures containing C, O, Zn, Mg, and Si, were predominantly detected (Figure 10).

Following the obtained results, XRD analyzes were performed on the two samples showing the highest and lowest strength (Figure 11). The XRD analyses of (a) AA6013+ 3% SiC composite welded at 110 A, and (b) of AA6013+ 6% SiC composite welded at 130 A. It was found that $(Al_{26}\ Si)_{0.148}$ and $Al_{0.985}\ Cu_{0.005}\ Mg_{0.01}$ were formed in the weld zones of both specimens. $(Fe_{97}\ Mn_3)_{0.02}$ was found to be formed differently in the 6% SiC reinforced

specimen. Considering the chemical composition of both the main material and the welding wire, it is normal to form of these structures.

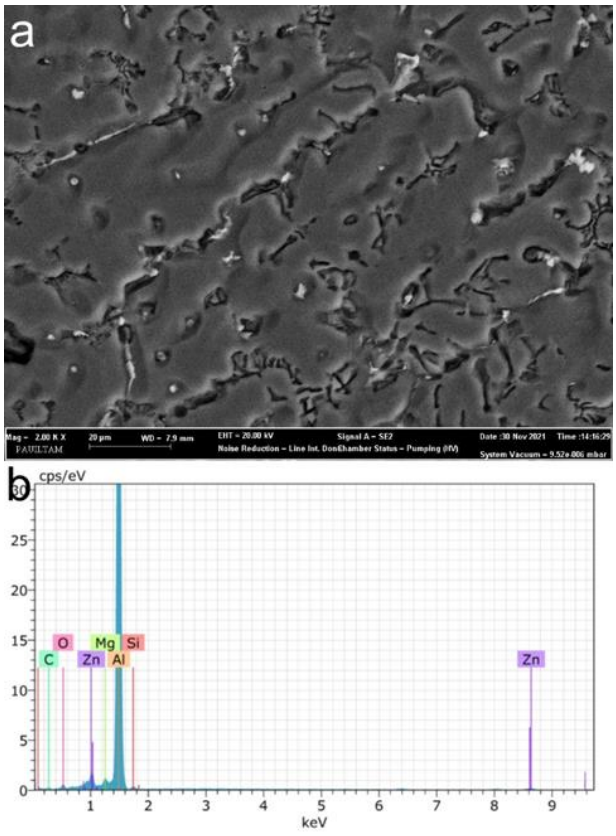

Figure 10. The FESEM microstructure image (a) and FESEM line analysis (b) of AA6013+ 9% SiC composite welded at 110 A

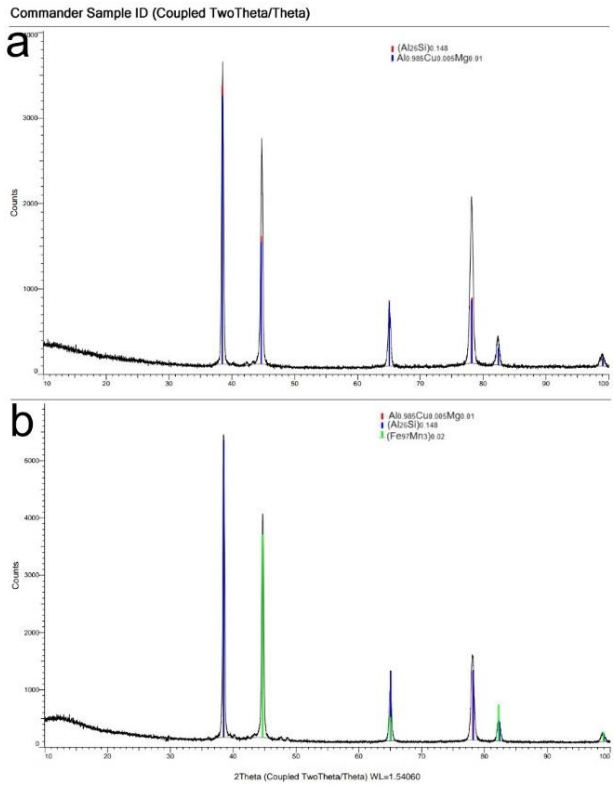

Figure 11. The XRD analyses of (a) AA6013+ 3% SiC composite welded at 110 A, and (b) of AA6013+ 6% SiC composite welded at 130 A.

4. DISCUSSION

Since the fusion zones frequently show coarse columnar grains as a result of the dominant heat conditions during the solidification of the weld metal, part strength reduces particularly as a result of fusion welding procedures. When compared to unwelded samples, welded samples' tensile strength can drop by up to 50% [18,19]. In this study, the mechanical characteristics of the unwelded and welded AA 6013 alloy under unreinforced and as-cast conditions, the tensile test results were close to each other. The mechanical property loss in welded samples was determined as 9.7% for Rm and 11.3% for Re. With the increase of heat input, the lowest values were obtained at 130 A welding current. These results show that the CMT method welding with current intensity and low heat input is suitable for unreinforced aluminum matrix composite.

When the mechanical properties of reinforced and welded composites were compared with the unreinforced and welded alloy, an increase in values ranging from 19% to 32% was obtained, except for the 6% SiC reinforced composite.

The porosity in a composite reinforced with coated Al_2O_3 particles was reduced by 15.45% in the work by Chandrasekar and Nagaraju [20] compared to the as-cast and unreinforced aluminum alloy. In addition, improvements of 15,2%, 23%, and 31,25% in hardness, tensile strength, and impact strength, respectively, were made. Aluminum 6063 MMCs reinforced with Al_2O_3, TiO_2, and SiC have higher tensile strength, hardness, and yield strength than pure AA 6063, and all these properties get better as the percentage of reinforcing particles increases, according to Shuvho et al. [21]. In this study, mechanical properties were improved with 3% and 9% SiC reinforcement. However, the most interesting result of the study is that welded with CMT while Rm and Re both decreased in the unreinforced specimens with welding process, except AA6013+6% SiC specimen, all welded SiC reinforced composites showed higher strength at all heat input values. This is a remarkable and innovative advancement. The mechanical properties did not increase in the welded samples with the increase of the reinforcement ratio. Considering the obtained results, it can be concluded that it is possible to obtain higher mechanical properties by keeping the reinforcement rate low with the CMT method which provides low heat input.

5. CONCLUSION

In this study, three distinct composites with aluminum AA 6013 matrix and 3%, 6%, and 9% SiC reinforcement by weight were produced using the vortex-route method. The cast samples were joined using CMT welding technique current intensities of 110, 120, and 130 A. The results of the studies carried out are summarized below:

With increasing heat input, the strength of the weld seam of the unreinforced material in the as-cast condition increased.

With increasing heat input, the strength of the weld seam of SiC reinforced AMCs decreased.

The CMT method resulted in higher weld seam strength than the unreinforced material.

As a result, strength values vary in different welding methods and different heat inputs, depending on the ratio of the

reinforcement material. By using 3% reinforcement material instead of 9%, more durable structures can be obtained at lower heat inputs.

ACKNOWLEDGEMENT

This study was supported by the Scientific Research Coordination Unit of Pamukkale University under project number 20FEBE041. The authors would like to thank Fronius Istanbul International for carrying out the welding operations.

REFERENCES

[1] N. Chawla, K. K. Chawla, Metal Matrix Composites, 2nd ed., Springer, New York, 2013, pp. 336–350.

[2] A. Ulukoy, M. Topçu, S. Tasgetiren, "Experimental investigation of aluminum matrix functionally graded material: Microstructural and hardness analyses, fretting, fatigue, and mechanical properties, Proceedings of the Institution of Mechanical Engineers, Part J: Journal of Engineering Tribology", vol. 230, no. 2, pp. 143–155, 2016, DOI: https://doi.org/10.1177/1350650115594405 .

[3] A. Ulukoy, M. Topçu, S. Tasgetiren, "The effect of aging treatments on wear behavior of aluminum matrix functionally graded material under wet and dry sliding conditions", Materialwissenschaft und Werkstofftechnik, vol. 42, no. 9, pp. 806–811, 2011, DOI: https://doi.org/10.1002/mawe.201100784

[4] M. Arumugam, M. S. Omkumar, M. Vinayagam, "Mechanical and Tribological characteristics of AA6082/ZrB2 composites", Materials Testing, vol. 63, no. 10, pp. 962-965, 2021, DOI: https://doi.org/10.1515/mt-2020-0111 .

[5] T. Singh, S. K. Tiwari, D. K. Shukla, "Mechanical and microstructural characterization of friction stir welded AA6061-T6 joints reinforced with nano-sized particles", Materials Characterization, vol. 159, pp. 1-14, 2020, DOI: https://doi.org/10.1016/j.matchar.2019.110047 .

[6] P. Bassani, E. Capello, D. Colombo, B. Previtali, M. Vedani, "Effect of process parameters on bead properties of A359/SiC MMCs welded by laser", Composites Part A: Applied Science and Manufacturing, vol. 38, no. 4, pp. 1089–1098, 2007, DOI: https://doi.org/10.1016/j.compositesa.2006.04.014 .

[7] C. G. Pickin, K. Young, "Evaluation of cold metal transfer (CMT) process for welding aluminium alloy, Science and Technology of Welding and Joining", vol. 11, no. 5, pp. 583–585, 2006, DOI: https://doi.org/10.1179/174329306X120886 .

[8] S. Selvi, A. Vishvaksenan, E. Rajasekar, "Cold metal transfer (CMT) technology-An overview", Defence technology, vol. 14, no. 1, pp. 28–44. 2018, DOI: https://doi.org/10.1016/j.dt.2017.08.002 .

[9] P. Kah, R. Suoranta, J. Martikainen, "Advanced gas metal arc welding processes", Int J Adv Manuf Technol, 67, 655-674, (2013).

[10] F. Kahraman, G. M. Gençer, C. Yolcu, A. D. Kahraman, M. E. Dilbaz, "Soğuk metal transfer (CMT) ve darbeli soğuk metal transfer (darbeli CMT) kaynak işlemleri ile birleştirilmiş AA5754 alüminyum alaşımının mikroyapi ve mekanik özelliklerinin karşılaştırmali olarak incelenmesi", DEU Mühendislik Fakültesi Fen ve Mühendislik Dergisi, 20(59), 625-636, (2018).

[11] K. Liu, X. Jiang, S. Chen, T. Yuan, Z. Yan, "Effect of SiC addition on microstructure and properties of Al–Mg alloy fabricated by powder and wire cold metal transfer process", Journal of Materials Research and Technology, 17, 310-319, (2022).

[12] Y. Fan, F. Chen, S. Cao, Y. Hu, R. Xie, "Effect of coating submicron-sized La2O3 particles on regulating grain structure and mechanical properties of 6061 aluminum alloy CMT welded joints", Materials Today Communications, 107764, (2023).

[13] E.F.A. Zeid, "Mechanical and electrochemical characteristics of solutionized AA 6061, AA6013 and AA 5086 aluminum alloys", Journal of Materials Research and Technology, 8(2), 1870-1877, (2019).

[14] S. Aytekin, "Analysis of the microstructure and hardness properties of aluminum matrix composite material reinforced with nano Al2O3 particles using different currents and forms of welding", Master's thesis, Pamukkale Üniversitesi Fen Bilimleri Enstitüsü, (2021).

[15] J.A. Taylor, "The effect of iron in Al-Si casting alloys", In 35th Australian Foundry Institute National Conference, Vol. 31, pp. 148-157, (2004).

[16] C.T. Wu, S.L. Lee, M.H. Hsieh, J.C. Lin, "Effects of Cu content on microstructure and mechanical properties of Al–14.5 Si–0.5 Mg alloy", Materials Characterization, 61(11), 1074-1079, (2010).

[17] A. Uluköy, "Pulsed metall inert gas (MIG) welding and its effects on the microstructure and element distribution of an aluminum matrix reinforced with SiC composite material", Materialwiss Werks (2017).

[18] A.K. Lakshminarayanan, V. Balasubramanian, K. Elangovan, K. "Effect of welding processes on tensile properties of AA6061 aluminium alloy joints". The International Journal of Advanced Manufacturing Technology, vol. 40, pp. 286-296, 2009, DOI: https://doi.org/10.1007/s00170-007-1325-0

[19] V. Balasubramanian, V. Ravisankar, G. Madhusudhan Reddy, "Effect of pulsed current welding on mechanical properties of high strength aluminum alloy". Journal of Advanced Manufacturing Technology, 36, 254-262, 2008, DOI: https://doi.org/10.1007/s00170-006-0848-0

[20] P. Chandrasekar, D. Nagaraju, "The Effect of Electroless Ni–P-Coated Al_2O_3 on Mechanical and Tribological Properties of Scrap Al Alloy MMCs". International Journal of Metalcasting, vol. 17, no. 1, pp. 356-372. (2022). https://doi.org/10.1007/s40962-022-00779-9

[21] M.B. Shuvho, M.A. Chowdhury, M. Kchaou, B.K. Roy, A. Rahman, M.A. Islam, "Surface characterization and mechanical behavior of aluminum based metal matrix composite reinforced with nano Al2O3, SiC, TiO2 particles". Chemical Data Collections, vol. 28, 100442, 2020). https://doi.org/10.1016/j.cdc.2020.100442

BIOGRAPHIES

Arzum Işıtan has a B.S. degree in Mechanical Engineering from Yildiz Technical University, a M.S. degree and a PhD degree in Mechanical Engineering from Pamukkale University. She has worked in Pamukkale University since 2002.

Dirim Bartuğ Göktürk obtained his BSc degree in manufacturing engineering from Pamukkale University (PAU). He works on machining and welded construction.

Volkan Onar has a B.S. degree and M.S. degree in Faculty of Technical Education, Metal Teaching from Gazi University, a Ph.D. degree in Metallurgy and Materials Engineering from Sakarya University. He has worked in Pamukkale University since 2012.